Catalysis Today 268 (2016) 46–59

Contents lists available at ScienceDirect

Catalysis Today

journal homepage: www.elsevier.com/locate/cattod

Electrochemically assisted synthesis of fuels by CO_2 hydrogenation over Fe in a bench scale solid electrolyte membrane reactor

Esperanza Ruiz*, Pedro J. Martínez, Ángel Morales, Gema San Vicente, Gonzalo de Diego, José María Sánchez

Centro de Investigaciones Energéticas, Medioambientales y Tecnológicas (CIEMAT), Av. Complutense, 40, 28040 Madrid, Spain

ARTICLE INFO

Article history:
Received 19 September 2015
Received in revised form 26 February 2016
Accepted 26 February 2016
Available online 11 March 2016

Keywords:
Solid electrolyte
Bench scale
CO_2 hydrogenation
Fe-TiO_2/YSZ
Electrochemical promotion

ABSTRACT

The electrochemically assisted synthesis of fuels by CO_2 hydrogenation was studied over a cheap, widespread and non-precious Fe catalyst in a bench scale oxygen ion conducting membrane (YSZ) reactor. The studies were performed under conditions representative of potential practical application i.e., under atmospheric pressure, at relatively low temperatures and high gas flow rates, with varying H_2/CO_2 ratios and using gas compositions typical for postcombustion CO_2 capture exit streams and easily scalable catalyst-electrode configurations.

The Fe-TiO_2 catalyst film was deposited by "dip-coating" and characterised both after pre-reduction and after testing.

CO_2 conversion and selectivities to CH_3OH and C_2H_6O can be enhanced up to 4, 50 and 1.7 times, respectively, by electrochemically controlled migration of O^{2-} promoting ions to or from the catalyst surface.

The optimum temperature for the process was 325 °C. Lower gas flow rates favoured the synthesis of CH_3OH and C_2H_6O. CO_2 conversion and selectivities to CH_3OH and C_2H_6O showed a maximum for a stoichiometric H_2/CO_2 ratio of 3. Formation of C_3H_6 and CO is strongly favoured for a H_2/CO_2 ratio of 4 and 2, respectively, as a result of the increased and decreased hydrogen availability in the reaction system.

1. Introduction

Due to the increase in CO_2 atmospheric levels and the diminishing fossil fuel resources arising from wide spread production of energy by fossil fuels combustion, valorisation of CO_2 emissions to clean fuels is viewed as a complementary strategy to capture and storage for an effective quantitative reduction of the CO_2 emissions, allowing their recycling and, therefore, a more sustainable use of the energy resources. Chemical recycling of carbon dioxide from combustion power plants, as an energy carrier, can be accomplished via its capture and subsequent hydrogenation to renewable, useful and environmentally neutral fuels (methane, methanol, dimethyl ether, etc.), provided that any available renewable energy source (wind, solar or hydraulic) is used for both production of necessary hydrogen (by water electrolysis) and chemical conversion of CO_2. Moreover, it has been foreseen that increasing amounts of cheap CO_2 will be available from carbon sequestration in the near future. In this way, carbon dioxide can be chemically converted from a harmful greenhouse gas causing global warning into a valuable, renewable, environmentally neutral and inexhaustible fuel source for the future [1–4].

Two main reactions can occur on co-feeding CO_2 and H_2 over a hydrogenation catalyst:

$$x\,CO_2 + (2x - z + y)H_2 \rightarrow C_xH_yO_z + (2x - z)H_2O \quad (1)$$

$$CO_2 + H_2 \rightarrow CO + H_2O \triangle G^{\circ} = 19.9\,kJ\,mol^{-1} \quad (2)$$

The former is the synthesis reaction resulting in the formation of hydrocarbons and/or oxygenates (alcohols or ethers). The latter is the reverse water gas shift (RWGS) reaction.

Most studies on conventional catalytic hydrogenation of CO_2 to fuels, such as methanol and dimethyl ether, have been accomplished using fixed-bed reactor configurations [3] of metal or metal oxide based catalysts supported on metal oxides [5] and at high pressures [6] to favour the CO_2 hydrogenation reaction. Electrochemical promotion is reported to be a very powerful tool, especially suitable for activation of very slow processes [7]. These processes if realized with conventional catalytic technologies need either extreme operating conditions (very high pressures and tem-

* Corresponding author.
E-mail address: esperanza.ruiz@ciemat.es (E. Ruiz).

http://dx.doi.org/10.1016/j.cattod.2016.02.025
0920-5861/

peratures) or long retention times [7], as seems to be the case for catalytic CO_2 hydrogenation. In fact, CO_2 adsorption and activation have been suggested to be the rate limiting step in CO_2 hydrogenation [5,8,9]. Therefore, operation of conventional catalysts at higher pressures results in an increased amount of adsorbed CO_2, and, hence, in an increase of reaction rate. However, electrochemical promotion of catalysis allows increasing the surface coverage of chemisorbed CO_2 species, giving rise to a concomitant increase in reaction rate and allowing the operation of the catalyst at lower pressures, which may result in energy savings.

Electrochemical promotion of catalysis (EPOC), by coupling electrochemistry to catalysis, has been considered as an alternative approach to classical chemical promotion of catalyst by electrochemically supplying and controlling the concentration of a promoter on an active metal catalyst surface. The application of small currents or potentials between a metal catalyst which is in contact with a solid electrolyte, which acts as a source of promoter species, and a counter electrode results in the migration of promoting species to or from the catalyst surface, allowing increasing the catalytic activity for the CO_2 hydrogenation reaction and modifying the selectivity to the desired products, as well as to simultaneously monitor and control the reaction during the process [4,9]. However, there are few previous studies of electrochemically promoted catalytic CO_2 hydrogenation. It has been studied over Cu on $SrZr_{0.9}Y_{0.1}O_{3-\alpha}$ (a proton conductor) [8], Pt on YSZ (an O^{2-} conductor) [5,10], Pd on YSZ or Na-βAl_2O_3 (a Na^+ conductor) [11], Rh on YSZ [5,12], Cu on TiO_2-YSZ [5], Ru on YSZ, Na-βAl_2O_3, K-βAl_2O_3 (a K+ conductor) or BZY (a proton conductor) [13–17], Ni or Ru impregnated carbon nanofibers on YSZ [18] and Ni on K-βAl_2O_3 [19]. In addition, these studies have been carried out at lab scale [8,10–19] and using reactor configurations (discs) [8,10,13–19], costly metals (Pt, Pd, Ru, Rd, etc.) [10–17], metal film preparation methods [8,10–12,18] and simplified gas compositions (H_2 and CO_2 diluted in He or N_2) [5,8,10–19] which are not representative of the potential practical application of the technology to real postcombustion CO_2 capture exit streams.

According to literature [7,20,21], to foster the ultimate utilization of electrochemical promotion of catalysis in commercial reactors, some challenges need to be addressed:

a.) Material cost minimization. Moving from thick catalyst films (0.1–5 mm thick), mostly made via paste deposition of high cost materials (noble metals) which lead to poor material utilization (metal dispersion below 0.01%) and low surface area, to thin (on the order of few nm thick) catalyst electrodes or dispersed catalysts that are sufficiently active, robust and inexpensive so as to be deployed in practical reactors. The use of less expensive catalysts (non-noble metals) and electrolyte systems is also needed. Commercially available materials and semiproducts should be used [20,21].

b.) Devising efficient and compact reactor design with easiness of electrical connection [20,21].To simplify reactor design and to make scale-up of electropromoted reactors easier, it is necessary to use configurations (multitubular, monoltithic, etc.) which would be susceptible of application in available devices (fixed bed conventional flow reactor), such as bipolar systems in combination with a single chamber reactor.

c.) The research focus has to be shifted from lab-scale, fundamental research, to more applied research (pilot plant scale tests, development of necessary catalyst manufacturing techniques etc.) [7].

d.) To verify the electrochemical promotion of catalysis in larger scale reactors at larger scale throughputs and in continuous mode of operation [7].

Therefore, there were some scale-up facets, such as operation at high flow rates, under realistic gas compositions and using catalyst-electrode configurations easily adaptable to the existing devices (conventional flow reactors), that need to be tackled in more depth for the potential practical application of this technology [7,20,21]. Moreover, there are also several aspects regarding the practical application of the technology, such as cost minimization, durability, useful lifetime, etc. which have not yet been addressed in detail [7,20,21].

We have recently reported various bench-scale studies of electrochemically assisted CO_2 hydrogenation to valuable hydrocarbon and oxygenated fuels over Pt [22] and Cu [23] on K-βAl_2O_3 and over Pt, Ni and Pd on YSZ [24]. These studies were carried out at high gas flow rates, under atmospheric pressure, at relatively low temperature and using gas compositions representative of CO_2 capture exit streams and tubular configurations easily adaptable to the existing catalytic devices (conventional flow reactors) and prepared by easily scalable procedures.

In the present work, we extend the study to other electrochemical catalyst systems, more specifically to Fe-TiO_2 on YSZ (an O^{2-} conductor). This system is based on a cheaper metal than Pt [22], but was also prepared by "dip-coating", which is thought to allow obtaining a thinner metal film than the "electroless" method used to deposit other non-noble metals, such as Cu [23] and Ni [24], which cannot be deposited by "dip-coating". Therefore, this study may contribute to decrease material cost for the process and to the development of the necessary catalyst manufacturing technique, which may have an impact in the potential practical application of the technology.

This work presents, to the extent of our knowledge for the first time, a bench-scale study of electrochemically promoted synthesis of renewable fuels by CO_2 hydrogenation over a cheap, widespread and non-precious Fe catalyst on $-TiO_2$/YSZ. This study was performed using only one-tube solid oxide cell configuration, but it could be envisaged to upscale the reactor design in a modular multitubular solid oxide cell configuration [25] with only two external connecting wires, which would be easily adaptable to available conventional flow reactors (fixed bed) and may simplify electrical supply to the electropromoted system.

In this study, Au was used for the counter electrode and connecting wires, given that it has been reported to be catalytically inactive for the CO_2 hydrogenation reaction [5,13], in order to ascribe the observed electrocatalytic behaviour to the Fe catalyst only. However, with a view of potential application, the use of other cost effective and easily available counter electrodes (stainless steel mesh/sheet, composites, etc.) and connection wires should be considered.

The use of a wireless electrochemical promotion approach, which is reported [26] to allow controlling the migration of oxide anion species through the solid electrolyte by controlling the oxygen chemical potential difference between both electrodes without the need of using connection wires, could also result in a simple configuration for upscaling the proposed catalyst system in a double chamber configuration with the counter electrode exposed to oxygen atmosphere.

The present study was performed at high flow rates, under atmospheric pressure, at relatively low temperatures and using concentrated CO_2 streams, meant to represent exit streams of post-combustion CO_2 capture plants (commercial amine plants) and H_2/CO_2 ratios from 2 to 4 to consider the effect of a discontinuous H_2 flow, as the H_2 needed for CO_2 hydrogenation may be discontinuously produced by water electrolysis only when electricity demand is low and from intermittent renewable energy sources [2,3]. It has been reported [3] that somewhat higher total CO_2 conversions (especially to CH_4) could be possible by using higher H_2/CO_2 ratios,

but the most efficient use of available H_2 occurs at lower H_2/CO_2 ratios.

Reactions conditions of temperature, flow rate and H_2/CO_2 ratios were varied to evaluate their influence on the extent of the electrochemically assisted CO_2 hydrogenation reaction and on the selectivity to the different target oxygenated fuels.

2. Experimental

2.1. Electrochemical catalyst

The electrochemical catalyst evaluated in the present work consisted of a thin Fe film (catalyst-working electrode), coated on a TiO_2 intermediate layer (used to improve electronic conductivity of the electrocatalyst), both deposited by dip-coating on the outer surface of a 26-mm-i.d., 100-mm-long, 1–2-mm-thick YSZ tube open on both sides.

A gold counter electrode was painted on the inner side of the tube to perform polarizations.

Au was chosen as the auxiliary electrode material because it is reported [5,13] to be inert for the CO_2 hydrogenation reaction.

The Au counter electrode was prepared by painting the inner side of the YSZ tube with a gold paste (HERAEUS-C5729). The deposited paste was dried at 150 °C during 10 min, heated to 850 °C at a controlled rate and, finally, annealed at 850 °C during 10 min.

Fe catalytic and intermediate TiO_2 layers have been also coated on the outer surface of the YSZ tube after deposition of the Au counter electrode on the inner side of the tube. Both open ends of the YSZ tube were plugged in order to avoid adding active catalyst particles to the counter electrode side.

Firstly, substrates were cleaned with absolute ethanol in an ultrasonic bath, rinsed with absolute ethanol and dried in an oven at 90 °C during 30 min.

Titanium dioxide has been deposited by sol-gel technique, using a precursor solution that contains water, ethanol, hydrochloric acid and tetrabutyl orthotitanate in a molar ratio 1/14/0.5/1. Withdrawal speed varied from 15 to 25 cm/min. Coatings have been thermally cured at 500 °C during 30 min.

Iron oxide has been deposited by dip-coating, withdrawing substrate from a precursor solution composed of 2-(2-aminoethylamino) ethanol, ethanol and ferrous nitrate, according to European patent EP1321539 [27], at speeds from 15 to 25 cm/min. Coatings have been thermally cured at 500 °C during 30 min.

The main role of TiO_2 intermediate layer is to enhance electronic conductivity of the Fe film which, as indicated above, was deposited as iron oxide and, as will be explained later, after reduction in H_2 at 400° C was mainly composed by metallic Fe and Fe_3O_4.

It has been reported, that under oxidizing conditions, TiO_2 alone exhibits mixed electronic -ionic (O^{2-}) conductivity and can lead to pronounced electrochemical promotion of oxidation reactions [28] and, in some cases, may protect active metal (Rh) from oxidation (by lowering the stability of potentially formed surface Rh oxides) under conditions (anodic polarization) where otherwise will be oxidized [29]. However, under the strongly reducing conditions of the present investigation, the conductivity of TiO_2 is entirely electronic [28] and the main role of TiO_2 is only to enhance the electronic conductivity of the Fe film.

2.2. Catalyst characterisation

A small fragment of the electrochemical catalyst was characterized, both after reduction and after testing, by Scanning Electron Microscopy (SEM), X-Ray Diffraction (XRD) and X-ray Photoelectron Spectroscopy (XPS) techniques.

The morphology of the catalyst film was investigated via SEM using a HITACHI SU6600 FEG-SEM instrument with ZrO/W emission type of 1–30 kV (100 V steps) of accelerating voltage and 3 nm at 1 kV/1.2 nm at 30 kV of resolution.

XRD patterns of the catalyst-working electrode films were recorded on a PHILIPS "Xpert-MPD" instrument using a Cu Kα X-ray source (45 kV and 40 mA), a 2θ range of 15–75°, a step size of 2θ = 0.03° and a step time of 2 s.

The surface chemical composition of the catalyst electrode film was examined by XPS using a Perkin-Elmer PHI 5400 System equipped with a Mg Kα ($h\nu$ = 1253.6 eV) excitation source running at 15 kV and 20 mA and having a beam diameter of 1 mm. Base pressure in the analysis chamber was maintained at about 10^{-9} Torr. The pass energy was set at 89.5 eV for general spectra (0–1100 eV) and at 35.75 eV for high resolution spectra. The energy scale was referenced to the carbon 1s signal at 285.0 eV.

2.3. Experimental set-up

Electrochemically assisted CO_2 hydrogenation over Fe-TiO_2 catalyst film was studied in a bench-scale plant, described in detail elsewhere [22], which is able to treat up to 20 $m^3\ h^{-1}$ (at 273 K and 1 atm) of gas with temperatures ranging between 250 and 450 °C, at about atmospheric pressure.

The different gas constituents of a post-combustion CO_2 capture exit stream and hydrogen can be provided by mass flow controllers from bottled gases. Steam can be supplied by vaporising water fed into a boiler by a metering pump. The mixed wet gas is then preheated and directed to a fixed-bed down-flow quartz reactor, with 35 mm of diameter and 900 mm of length, heated by a three-zone electrical furnace. Polarization across the cell was measured and controlled via a potentiostat-galvanostat.

Gaseous products from the reactor were delivered through a heated transfer line to the gas analysis system in order to avoid condensation of any volatile products. Gas composition was simultaneously determined using a gas micro-chromatograph, and an NDIR CO_2/CO on line analyser [22], allowing the analysis of: H_2, N_2, CO, CH_4, CO_2, C_2H_2, C_2H_4, C_2H_6, C_3H_6, C_3H_8, methanol, dimethyl ether and ethanol.

2.4. Operating conditions and procedure

The electrochemical catalysts were properly situated in the reactor in order to lessen by-pass phenomena and to enhance catalyst-reactive gas contact. The electrical connections in the reactor were made from gold wires (HERAEUS), which is reported to be catalytically inert in the process [5]; therefore, all the potential-induced changes in catalytic activity and selectivity can be exclusively attributed to the metal film.

The Fe film was reduced in a stream of H_2 at 400 °C during 1 h [22], before performing the electrochemically assisted CO_2 hydrogenation experiments.

Open circuit potential was maintained during 30 min prior to each test to define a reproducible reference state. Electrochemically assisted hydrogenation tests were performed under H_2/CO_2 binary mixtures, at different applied potentials (between −2 and 2 V), H_2/CO_2 ratios (from 2 to 4), temperatures (225–400 °C) and flow rates (90–216 N $l\ h^{-1}$), in order to determine the effect of the utilized operating conditions on CO_2 conversion, efficiency of electrochemical promotion and selectivity to the different fuel products.

CO_2 hydrogenation tests were performed under H_2 and CO_2 binary mixtures; although a small amount of N_2 (about 0.5%) was added to the reaction gas mix as an internal standard. Accordingly

[20], CO_2 conversion (X_{CO_2}) and "CO_2 free selectivity" is defined as (3) and (4), respectively:

$$X_{CO_2} = \left(1 - \frac{[CO_2]_o \times [N_2]_i}{[CO_2]_i \times [N_2]_o}\right) \times 100 \quad (3)$$

$$S_i = \frac{n_i \times M_i}{\sum_{i=1}^{i=n} n_i \times M_i} \times 100 \quad (4)$$

where $[CO_2]_i$ and $[CO_2]_o$ are the corresponding CO_2 molar quantities at the inlet and outlet of the reactor. As well, $[N_2]_i$ and $[N_2]_o$ are N_2 molar quantities at the inlet and outlet of the reactor, respectively. Additionally, S_i is the selectivity to product i, n_i is the number of carbon atoms of product i and M_i is moles of product i, respectively.

The effect of polarization on catalyst performance for the CO_2 hydrogenation reaction was gauged in terms of CO_2 rate enhancement ratio (Eq. (5)) [22].

CO_2 rate enhancement ratio is defined as (Eq. (5)):

$$\rho CO_2 = \frac{rCO_2^p}{rCO_2^{up}} \quad (5)$$

where rCO_2^p and rCO_2^{up} are the CO_2 catalytic rates with (under application of a given potential V) and without (unpromoted reference state, under open circuit conditions, i.e., no potential application and measured open circuit potential almost equal to 0 V) electrochemical promotion, respectively.

According to literature [5,13,16], in the case of CO_2 hydrogenation on metal catalysts deposited on YSZ (an O^{2-} ion conductor), O_2 is not a reactant and, therefore, any positive potential-induced catalytic rate change is due to electrochemical promotion independently of the value of Faradaic efficiency. The same can be reasoned in the case of negative potential, because even if CO_2 is decomposed via O^{2-} removal from the catalyst surface, this does not lead to H_2O formation. In any case, the apparent Faradaic efficiency Λ [5], which is also commonly used to quantify the magnitude of electrochemical promotion, has been also calculated. The apparent Faradaic efficiency Λ [5] is defined from (6):

$$\Lambda_i = \frac{r - ro}{I/F} = \frac{\Delta r}{I/F} = \frac{\Delta r_i(mol/s) \times E_i}{I/F} \quad (6)$$

where r is the electropromoted rate and ro is the normal, open circuit catalytic rate (both in g-eq/s). Δr_i is the current- or potential-induced change in the catalytic rate of each product formation (mol/s) and E_i is the g-eq factor for each product formation reaction. In this study, Λ has been calculated for the main product obtained at each H_2/CO_2 ratios, i.e. Λ_{C2H6O} ($E_{C2H6O} = 6$), Λ_{C3H6} ($E_{C3H6} = 6$) and Λ_{CO} ($E_{CO} = 2$) for H_2/CO_2 ratios of 3, 4 and 2, respectively. F is the Faraday's constant, I is the applied current. The term I/F corresponds to the rate of ions (g-eq/s) supplied to catalyst according to the Faraday's law. Thus, $|\Lambda| = 1$ refers to pure Faradaic rate enhancement, and $|\Lambda| > 1$ implies electrochemical promotion.

The value of current efficiency (η_c) and energy cost (C_E) were calculated for each fuel product formation (methanol, ethanol and dimethyl ether) under different applied potentials and operating conditions, following the expressions (7) and (8), respectively:

$$\eta_c = \left\{(m_p/M_p) \times \nu_e/\nu_p \times F\right\}/(I \times t) \quad (7)$$

$$C_E = V \times F \times (\nu_e/\nu_p)/(\eta_c \times M_p) \quad (8)$$

where ν_e is the number of electrons transferred and ν_p is the stoichiometric coefficient in each product formation reaction. Additionally, m_p and M_p are the mass and molecular weight of product formed, respectively.

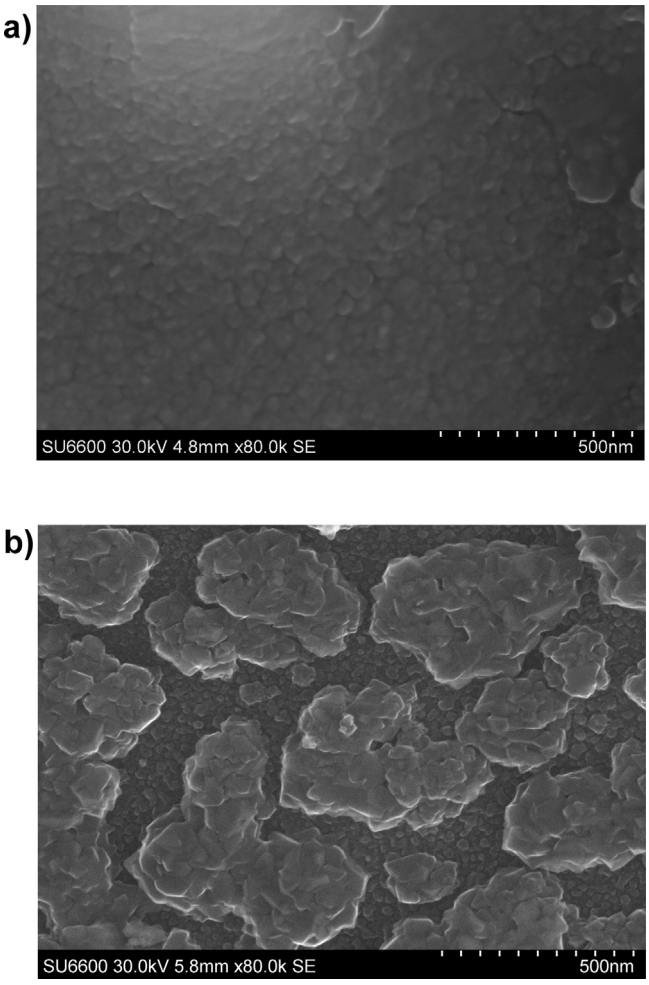

Fig. 1. SEM micrograph of the Fe catalyst-working electrode film: (a) after reduction, (b) after testing.

The carbon mass balance (relative difference between carbon mass at the reactor inlet and outlet) was also calculated for each test and resulted to be below 0.5% for all cases.

3. Results and discussion

3.1. Catalyst characterisation studies

As reported in literature [6,30–35], the utilised preparation technique determines also porous structure, surface morphology and particle size of the metal thin film and therefore the electrochemically assisted catalytic behaviour of the system. SEM micrographs of Fe catalyst-working electrode film, both as prepared and after reduction (a) and after testing (b), are shown in Fig. 1a and b, respectively. As can be observed in SEM image of the sample after reduction in Fig. 1(a), the obtained film seems to resemble a typical foam structure [36], suggesting that they are porous (allowing reactants and products diffusion), and continuous, as verified by electrical conductivity measurements. The Fe film thickness was also determined by SEM and resulted to be about 200 nm.

XRD spectra of the fresh (as prepared and reduced) and used (after exposure to reaction conditions) samples of Fe film are compared in Fig. 2. The peaks at $2\theta = 44.8^\circ$, 65.1° and 82.6°, in the XRD spectra of the as reduced sample, were identified as the typical diffraction peaks of Fe metal (JCPDS card no. 01-087-0722); whereas the rest of peaks were assigned to the YSZ solid electrolyte

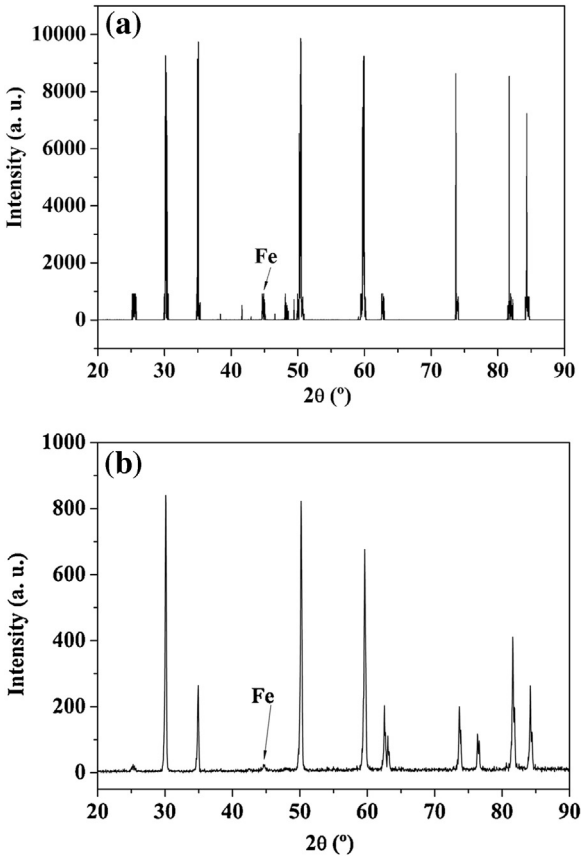

Fig. 2. XRD analysis of the Fe catalyst-working electrode film: (a) after reduction, (b) after testing.

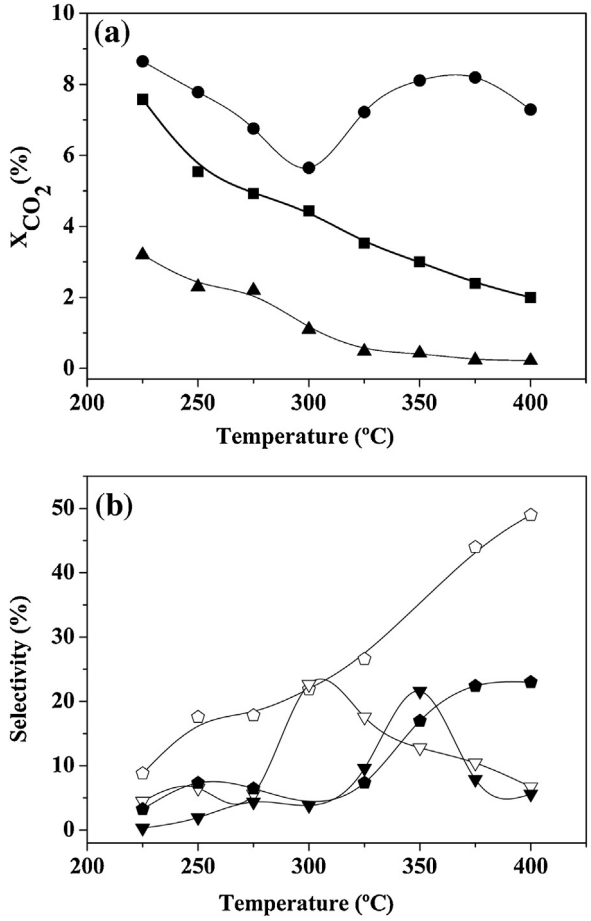

Fig. 3. Influence of temperature on (a) CO_2 conversion under open circuit conditions (■), upon negative polarization (−2 V) (●) and upon positive polarization (2 V) (▲) and on (b) selectivities to CH_3OH (▼, ▽) and C_2H_6O (⬟, ⬠) under open circuit conditions (filled symbols) and upon negative polarization (−2 V) (open symbols) over Fe-TiO_2/YSZ/Au. (225–400 °C, 90 l h^{-1}, H_2/CO_2 = 3).

(JCPDS card no. 98-008-9429) and to the TiO_2 intermediate layer (JCPDS card no. 98-009-2363). No peaks of iron oxides, or other phases, were detected for the sample after reduction.

The average crystallite size of the as reduced sample was evaluated from X-ray broadening of the main metallic Fe diffraction peak at 2θ = 44.815 by using the well-known Debey-Scherrer equation [37,38]. The average particle size resulted to be of about 38 nm. The catalyst film metal dispersion has been also estimated from the obtained particle diameter and resulted to be of about 3.2% [39].

The XPS analysis of the fresh (as prepared and reduced) sample revealed the presence of several superficial compounds that could not be identified by XRD, resulting in Fe being present mainly as Fe_3O_4 as shown by the appearance of peaks at a binding energy of about 711 eV in the Fe 2p3/2 spectra and at a binding energy of about 724.6 eV in the Fe 2p1/2 [40–43]. The appearance of a peak at 529.77 eV in the O1s spectra seems to confirm the presence of Fe_3O_4 in the as reduced sample.

Reflections of the rest of Fe_3O_4 phase were undetectable in the XRD pattern of the as reduced sample. This seems to indicate that the as-deposited and reduced Fe film could be almost XRD-amorphous or nanocrystalline.

According to literature [44], the reduction of iron catalyst by hydrogen is known to be a two or three-staged process. That is first Fe_2O_3 is reduced at 397 °C to Fe_3O_4, which is then reduced to metallic iron at 702 °C. According to catalyst characterization, initially deposited iron oxides were reduced to Fe_3O_4 and partly also to Fe during reduction in H_2 at 400 °C.

Some agglomerates can be observed in SEM image of the sample after testing (Fig. 1(b)), which are thought to be related with sintering of iron particles upon exposure to testing gas environment and not to the fact that the examined area is different in the case of the used sample. This fact seems to be confirmed also by XRD which revealed a loss of crystallinity, as can be deduced from the decrease of the intensity of XRD peaks associated with metallic Fe.

The XPS spectra of the used sample revealed also the coexistence of Fe oxides and oxides/hydroxides as resembled by the appearance of peaks at binding energies of about 710.3 eV in the Fe $2p_{3/2}$ spectra. The O1s spectra showed also that oxygen could be present as OH groups (38.7%) and Fe oxides (61.4%) as indicated by the appearance of peaks at binding energies of about 529.8 and 531.6 eV, respectively. These results suggest that Fe and or Fe_3O_4 could be oxidized/oxohydroxized under reaction conditions.

3.2. *Electrochemically assisted CO_2 hydrogenation tests*

3.2.1. *Effect of temperature*

Fig. 3(a) shows the effect of temperature on the conversion of CO_2 under open-circuit state and upon cathodic (−2 V) and anodic (+2 V) polarization conditions, at temperatures from 225 to 400 °C and using 90 l h^{-1} of total gas flow rate and a H_2/CO_2 ratio of 3.

Dimethyl ether, methanol, ethanol, CO and in lesser extent hydrocarbons (mainly C_2H_6 and C_3H_6), CH_4, formic acid and acetic acid were formed depending on polarization conditions and temperatures.

As can be observed in Fig. 3(a), under open circuit and positive polarization conditions, CO_2 conversion monotonically decreases as temperature increases for whatever value of applied potential.

This fact may be related to catalyst poisoning by carbon deposition over Fe and Fe_3O_4 which progressively blocks the active sites [44,45] or by oxidation of Fe_3O_4 to inactive Fe oxides (Fe_2O_3) [45] (during ongoing carbon deposition) or hydroxides ($Fe(OH)_3$) [46] (by OH^- [13] species resulting from O^{2-} ions thermally and/or electrochemically supplied to Fe surface).

Upon negative polarization CO_2 conversion decreases on increasing temperature up to 300 °C, also probably due to catalyst poisoning by carbon deposition, and then slightly increases with temperature, showing a maximum at about 350 °C, and after that, CO_2 conversion decreases on increasing temperature.

According to catalyst characterisation results, iron oxides were reduced to Fe_3O_4 and partly to metallic Fe during pre-reduction at 400 °C and subsequently oxidized to a less crystalline (amorphous) phase consisting of iron oxides and hydroxides upon exposure of the catalyst to the testing gas environment and operating conditions.

Iron oxides, which have been used as FT catalysts for many years, are also active in reverse water gas sift reaction (RWGS) (Eq. (2)) [47]. According to literature [48,49], active species for Fischer Tropsch (FT) reaction are generally obtained by the reduction of α-Fe_2O_3 via Fe_3O_4, i.e., the iron species derived from α-Fe_2O_3 seems to be the catalytic sites for FT-reaction. Moreover, during CO_2 hydrogenation, Fe_3O_4 phase is reported to disappear slowly and a new amorphous, probably oxidic phase is formed, which appears to be also active for the RWGS reaction [47].

In accordance with literature [47,50], CO_2 hydrogenation over Fe based conventional catalyst (unpromoted conditions) proceeds via a two-step process, with initial reduction of CO_2 to CO via RWGS reaction followed by conversion of CO via FT reaction. FT synthesis is reported [51] to produce both hydrocarbon and oxygenated products (oxygenates) by reducing CO with hydrogen on a suitable catalyst, such as iron supported on TiO_2 [49]. It has been reported [49] that on Fe-TiO_2 catalysts, both metallic and oxidic iron phases may play different roles in CO_2 hydrogenation. Iron oxides are necessary for the hydrogenation of CO_2 to from CO. Metallic iron is beneficial to form lower olefins in CO hydrogenation. Moreover, iron oxides are also active to form oxygenates (CH_3OH, C_2H_6O, etc.) from CO [51].

Another coexistent reaction is the CO_2 reduction to carbon. According to literature [44], CO_2 can be at least partially dissociated to CO on the Fe_3O_4 species and in part decomposed further to carbon, which may result in catalyst deactivation by deposition of carbonaceous material. Therefore, decomposition of adsorbed carbon dioxide (Eq. (9)) into carbon on magnetite species occurs in two steps (Eq. (10) and (11)). Simultaneously, Fe_3O_4 may capture the oxygen released by CO_2 and CO dissociation and converts itself into Fe_2O_3 (inactive for RWGS and carbon deposition), which may also result in catalyst deactivation. The amount of carbon on the surface of the catalyst may be considered an indication of the dissociative adsorption of CO_2. Propensity for CO_2 decomposition is reported to be higher over zirconium catalysts [44].

$$CO_2 + e \rightarrow CO_2{}^{*-}(ads.) \triangle G^\circ = 183.3\,kJ\,mol^{-1} \quad (9)$$

$$CO_2{}^{*-}(ads.) + e \rightarrow CO^*(ads.) + O^{2-} \triangle G^\circ = 257.2\,kJ\,mol^{-1} \quad (10)$$

$$CO^*(ads.) + e \rightarrow C^*(ads.) + O^{2-} \triangle G^\circ = 137.2\,kJ\,mol^{-1} \quad (11)$$

CO_2 conversion could decrease with temperature also as a result of the concomitant increase in the extent of carbon deposition and in the stability of the surface carbon species formed [52]. It has been reported [47,53] that at the beginning of the reaction (at low temperature), carbon deposition on the catalyst surface takes place dominantly with a little formation of CO. On increasing temperature, reverse water gas shift reaction yield increases and products from RWGS dominate during ongoing carbon deposition. Upon additional increase in temperature, the RWGS activity increases further and FT activity develops and is progressively stablished on the catalyst surface. CO yield increases with temperature via the RWGS reaction which is a reversible endothermic reaction. However, the dependence of hydrocarbon and oxygenates yield is under a compromise between higher driving force in activity and larger tendency to inert carbon deposition [47,52].

It has been reported [13] that under reducing conditions, as in the present case (binary mixture of H_2 and CO_2), it is likely that hydroxyl group anionic species (OH^-) are formed by reaction of hydrogen with electrochemically/thermally migrated O^{2-} species, which are reported [5] to have a short lifetime, on the catalyst surface. Therefore, in spite of the strongly reducing environment, Fe_3O_4 might be oxidized to inactive Fe hydroxides [46] by the hydroxyl species, contributing also to magnetite deactivation. The application of positive potentials (+2 V) results in O^{2-} supplying from solid electrolyte to the catalyst surface [5,13]. Therefore, the decrease in conversion values obtained for positive polarization could be also because upon application of positive potentials oxygen ions are transferred from the solid electrolyte to the Fe catalyst surface resulting in an increased Fe_3O_4 oxidation. In absence of polarization, i.e., under unpromoted conditions, although no electrical current passes across the cell, O^{2-} ions could also thermally migrate from the solid electrolyte to the catalyst surface as temperature increases, due to the increased ionic conductivity of the solid electrolyte at higher temperatures. In both cases CO_2 conversion decreases as temperature increases, because migration of O^{2-} to the catalyst surface increases with temperature as a result of the increased ionic conductivity at higher temperatures.

On the contrary, under negative polarization (−2 V), O^{2-} species are pumped away from the catalyst surface to the solid electrolyte YSZ, enhancing CO_2 dissociative adsorption to CO (Eq. (10)) and subsequent formed CO dissociation into surface carbon species (Eq. (11)) [6,54,55], as well as direct CO_2 reduction to carbon species (Eq. (12)). Therefore, the initial decrease on CO_2 conversion on increasing temperature observed is thought to be due to Fe poisoning by carbon deposition, given that the amount of surface carbon adsorbed on the catalyst surface is expected to increase with time and temperature [2]. As commented above on increasing temperature reverse water gas shift reaction (RWGS) activity increases. Under negative polarization (−2 V), upon increasing temperature ionic conductivity of the electrolyte, and therefore, O^{2-} removal from the catalyst surface, increases also, facilitating further RWGS reaction by the electrochemically enhanced CO_2 dissociative adsorption to CO and subsequent CO hydrogenation to oxygenates and hydrocarbons. Therefore, the increase in CO_2 conversion levels observed under negative polarization could be due to the improved CO_2 dissociation, via O^{2-} abstraction.

$$CO_2{}^{*-}(ads.) + 4e \rightarrow C^*(ads.) + 2O^{2-} \triangle G^\circ = 394.4\,kJ\,mol^{-1} \quad (12)$$

Given that there is no O_2 in the gas phase, the reported [5] short lifetime of the O^{2-} species on the catalyst surface under reducing conditions and the limited O^{2-} capacity of the YSZ support, the stability of the solid electrolyte (YSZ) under working conditions can be questionable. However, the O^{2-} species in the solid electrolyte can be replaced by pumping of O^{2-} species, resulting from electrochemical reduction of CO_2/adsorbed CO on the corresponding electrode (gold or iron), to the solid electrolyte, allowing the solid electrolyte to be stable under EPOC working conditions. In fact, it has been previously demonstrated [13] that, upon positive polarization, O^{2-} ions could be generated at the gold counter electrode by electrochemical reduction of CO_2 with the subsequent formation of CO adsorbed on the surface and also possibly by subsequent electrochemical reduction of the adsorbed CO species forming C surface species, followed by removal of O^{2-} from the gold film surface to the solid electrolyte. Upon negative polarization, O^{2-} ions can be

originated by same phenomena taking place at the iron catalyst electrode.

Fig. 3(b) shows the effect of temperature on the selectivity to the target oxygenated products (CH_3OH and C_2H_6O) under open-circuit state and upon cathodic (−2 V) polarization conditions, at temperatures from 225 to 400 °C and using 90 l h^{-1} of total gas flow rate and a H_2/CO_2 ratio of 3.

The selectivity to CH_3OH exhibited a maximum at a given temperature and then decreased with the temperature increment, which agree with the fact that the equilibrium conversion of CO_2 to methanol decreases as temperature increases [49,50]. A H_2/CO_2 ratio of 3 matched with the theoretical stoichiometry in the methanol and dimethyl ether synthesis reactions by CO_2 hydrogenation according to Eqs. (13)–(14), and thus they are thermodynamically favoured under these conditions. Moreover, C_2H_6O can be also formed by dehydration (Eq. (15)) of CH_3OH.

In fact, as reported by literature [57], methanol converted to dimethyl ether at 250–300 °C and both methanol and dimethyl ether are reported to be transformed into hydrocarbons at temperatures about 400 °C [57], where RWGS (Eq. (2)) and methanation (Eq. (16)) reactions are also favoured [5].

$$CO_2 + 3H_2 \rightarrow CH_3OH + H_2O \triangle G^{\circ} = -9.1\ \text{kJ mol}^{-1} \quad (13)$$

$$2CO_2 + 6H_2 \rightarrow C_2H_6O + 3H_2O \triangle G^{\circ} = -36.8\ \text{kJ mol}^{-1} \quad (14)$$

$$2CH_3OH \rightarrow C_2H_6O + H_2O \quad (15)$$

$$CO_2 + 4H_2 \rightarrow CH_4 + 2H_2O \triangle G^{\circ} = -130.7\ \text{kJ mol}^{-1} \quad (16)$$

In the absence of surface oxygen ions (no polarization) and under anodic (+2 V) polarization, CO_2 conversion shows a maximum (around 7% and 3%, respectively) at about 225 °C. Cathodic (−2 V) polarization leads to a slight increase in CO_2 conversion which reaches about 8% at an higher temperature of about 350 °C, where the effect of electrochemical promotion is more pronounced due to the increased ionic conductivity of the solid electrolyte at higher temperatures.

In the absence of surface oxygen ions (no polarization), the selectivity to CH_3OH attained a maximum of about 19% around 350 °C, then decreased with the temperature increment, whereas selectivity to C_2H_6O increased with temperature from about 4% at 225 °C to around 20% at 400 °C. Application of negative polarization (−2 V) leads to a slight increase in the maximum of CH_3OH selectivity (20%), and it is obtained at lower temperature (around 300–325 °C). Selectivity to C_2H_6O is noticeably electrochemically enhanced over the studied temperature range, showing the same tendency against temperature, increasing from about 10% at 225 °C to around 50% at 400 °C.

As commented above, negative polarization results in higher levels of CO_2 conversion and selectivity to CH_3OH and C_2H_6O with respect to that under open circuit conditions, because CO_2 dissociative adsorption, which is reported to be the limiting step in CO_2 hydrogenation [5,8,9,58], is facilitated by oxygen removal from the catalyst surface.

Results obtained at different temperatures revealed that CO_2 conversion and selectivity to the different target products were maximum at temperatures around 325–350 °C. Therefore, a temperature value of 325 °C was selected for subsequent experiments.

3.2.2. Effect of potential

The steady state effect of polarization on the behaviour of Fe-TiO_2/YSZ/Au was investigated through potentiostatic experiments performed at different H_2/CO_2 ratios (2–4) at the selected temperature of 325 °C and 90 l h^{-1}.

In order to consider the less favourable, although more realistic, conditions associated with a discontinuous flow of renewable H_2 [2], the behaviour of the catalyst was also studied using H_2/CO_2 ratios of 2 and 4, which correspond to a lack and an excess of H_2, respectively, in relation to the stoichiometry of the target products (CH_3OH and C_2H_6O) formation reactions ((Eq. (10)) and (Eq. (11)), respectively).

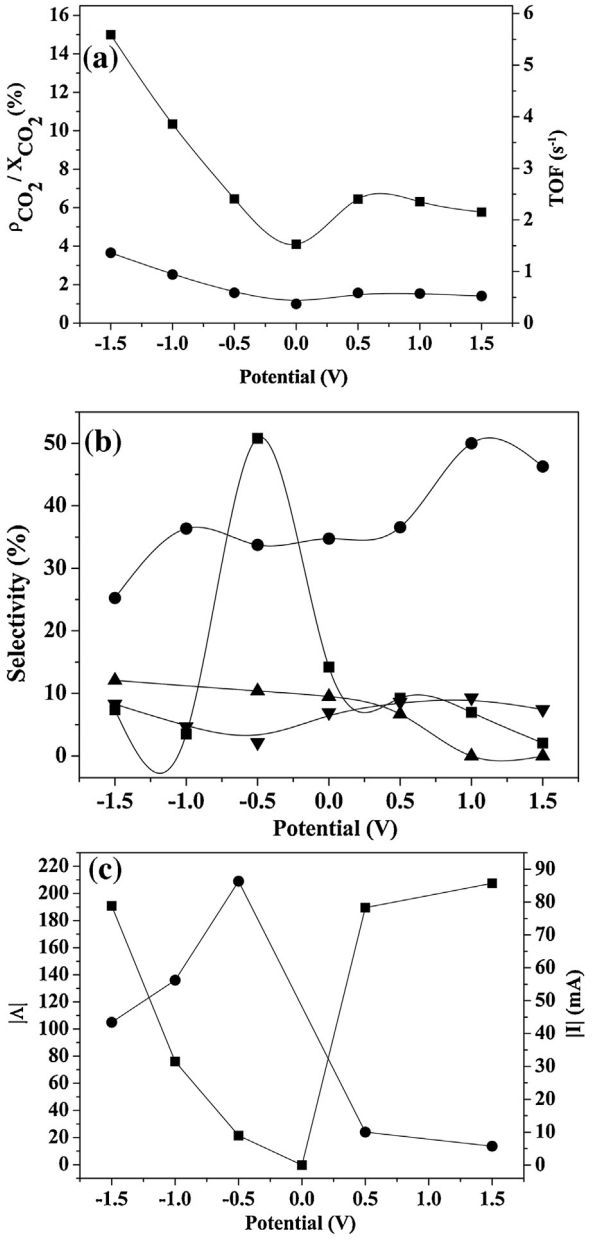

Fig. 4. Influence of the applied potential on (a) CO_2 conversion/TOF (■) and CO_2 rate enhancement ratio (●), on (b) selectivities to CH_3OH (■), C_2H_6O (●), CO (▲) and C_2H_5OH (▼) and on (c) current (■) and apparent faradaic efficiency (●) over Fe-TiO_2/YSZ/Au. (325 °C, 90 l h^{-1}, H_2/CO_2 = 3).

The steady state response of CO_2 conversion, Turn Over Frequency (TOF) and CO_2 rate enhancement ratio to different applied catalyst potentials (between −1.5 and 1.5 V) is displayed in Fig. 4a at 325 °C and 90 l h^{-1} and using a H_2/CO_2 ratio of 3. Fig. 4b shows the effect of applied potential on the selectivity to CO, CH_3OH, C_2H_6O, and C_2H_5OH, respectively, whereas, Fig. 4c shows the variation of apparent faradaic efficiency ($|\Lambda|$) and current with applied potential, under the same conditions.

As commented above, for H_2/CO_2 ratios of 3, the hydrogenation of CO_2 over Fe-TiO_2/YSZ/Au gives rise mainly to the formation of methanol (Eq. (13)), dimethyl ether (Eq. (14)), ethanol (Eq. (17)) and CO (Eq. (2)), but (not shown) hydrocarbons (mainly C_2H_6 and

C_3H_6), CH_4, formic acid and acetic acid were also detected to be formed.

$$2CO_2 + 6H_2 \rightarrow C_2H_5OH + 3H_2O \quad (17)$$

Moreover, C_2H_5OH can be also formed by hydrogenation (Eq. (18)) and hydration (Eq. (19)) of CH_3OH.

$$2CH_3OH + 3H_2 \rightarrow C_2H_5OH + H_2O \quad (18)$$

$$2CH_3OH + H_2O \rightarrow C_2H_5OH \quad (19)$$

In fact, a H_2/CO_2 ratio of 3 is about the stoichiometric ratio required for CH_3OH, C_2H_5OH and C_2H_6O production and thus these reactions are thermodynamically favoured and are in competition over the catalyst surface under these conditions.

In this case, CO_2 hydrogenation is considerably influenced by the applied potential, with selectivities to C_2H_6O, C_2H_5OH, CO and CH_3OH up to about 47%, 10%, 12% and 50%, respectively. CO_2 rate enhancement ratio values are rather low (up to about 4) with CO_2 conversions up to 15%. TOF exhibited higher values (up to 5.5 s^{-1}) than those reported [5] for a similar electrochemical catalyst ($Cu/TiO_2/YSZ/Au$), which evidenced a better performance of the present catalyst system.

As can be observed in Fig. 4c, $|\Lambda| > 1$ for whatever value of applied potential. The maximum value of $|\Lambda|$ is obtained for −0.5 V and resulted to be 209. Such a high apparent Faradaic efficiency is a distinguishing feature of electrochemical promotion vs. electrocatalysis [9].

The catalyst showed an "inverted volcano type" electrochemical behaviour, i.e., CO_2 rate enhancement ratio exhibits a minimum at certain potential (at around 0 V) [9,59] (Fig. 4a). This behaviour can be attributed to the increase of hydrogen (electron donor) and CO_2 (electron acceptor) adsorption strength and surface coverage upon positive and negative polarization, respectively, as expected from the rules of electrochemical promotion [5,13]. The difference in the rate enhancement observed for negative and positive potential application can be attributed to the difference in the chemisorption propensity of CO_2 and hydrogen on Fe. CO_2 is less easily adsorbed on Fe compared to H_2, thus enhancement of its chemisorption via negative polarization is expected to have a more significant impact on the rate [11].

However, selectivity to C_2H_6O diminished with potential decrease (Fig. 4b), i.e., an electrophobic electrochemical behaviour is observed, while selectivity to CO increases with decreasing catalyst potential (Fig. 4b), showing an electrophilic electrochemical behaviour [9,59].

As can be deduced also from Fig. 4b, the selectivity to C_2H_5OH follows opposite trends vs. applied potential with respect to that of CO selectivity, whereas C_2H_6O production is strongly enhanced at positive potentials, being a competition for the formation of the different hydrogenation products over the catalyst surface. In fact, as shown in Fig. 4b, with increasing catalyst potential by approximately 1 V (from 0 to 1 V), the selectivity to C_2H_6O increases by 1.4 times. As can be also observed in Fig. 4b, with decreasing catalyst potential by about 1.5 V (from 1 to −0.5 V), CO selectivity increases by about 100 times and C_2H_5OH selectivity decreases by about 2 times.

As can be observed also in Fig. 4b, the optimum applied potential for CH_3OH formation is about −0.5 V, which corresponds with an enhancement in their selectivity of up to about 4 times (with respect to unpromoted open circuit conditions). Increasing or decreasing applied potential from this value resulted in a decrease in CH_3OH selectivity, i.e., selectivity to CH_3OH exhibited a maximum at this potential, showing a "volcano type" electrochemical behaviour. C_2H_5OH exhibit a concomitant minimum at this potential, showing an "inverted volcano type" electrochemical behaviour, which corresponds with a decrease in C_2H_5OH formation of up to approximately 50%.

Chemisorption of reactive molecules on a catalyst surface is the previous step to any catalytic process. Chemisorption of an adsorbate on a metal gives rise to a real chemical bond, thus implying electron donation from adsorbate to metal or from metal to adsorbate. In the first case, the adsorbate is called electron donor (electropositive), whereas in the second, is called electron acceptor (electronegative). There is a certain scale of electronegativity or electron acceptor capacity, in which oxygen is one of the strongest electron acceptors. The concept of electropositive or electronegative is also valid for the promoter ions in charge of the phenomenon, being these cations (electropositive promoters) and anions (electronegative promoters), respectively [9].

The origin of the electrochemical activation relies on the modification of adsorption phenomena. In the electrochemical promotion, promoter species are ions which electrochemically migrate in a controlled manner from the support (solid electrolyte) to the metal. The migration of these ions are accompanied by that of the corresponding charge compensation ion, forming neutral surface dipoles which are distributed along the metallic surface giving rise to the ≪effective double layer≫. Formation of the effective double layer gives rise to a change in the work function of the metal catalyst (Φ), modifying its bond capacity which each reactive, and therefore its catalytic behaviour [9,59].

On the one hand, the increment in catalyst work function of the metal catalyst by addition of an electronegative promoter (O^{2-} for YSZ), via application of positive potentials, favoured the adsorption of electron donor species (H_2), because the electrode becomes positively charged (due to a defect of electrons), favouring the transfer of electrons from electron donor molecules, like H_2, to the catalyst electrode and thus the adsorption of the latter on the catalyst surface, whereas at the same time hindered the adsorption of electron acceptor species (CO_2 in this case), giving rise to an increase in H_2 (electron donor) coverage and to a decrease in the coverage of CO_2 (electron acceptor). The opposite occurs for application of negative potentials which results in the removal of O^{2-} promoter species from the catalyst electrode to the solid electrolyte, giving rise to a decrease of the catalyst work function, i.e., the electrode becomes negatively charged (due to an excess of electrons), which favours the transfer of electrons from the catalyst to electron acceptor molecules, like CO_2, and, thus, the adsorption of the latter on the catalyst surface, whereas at the same time hindered the adsorption of electron donor species (H_2 in this case), giving rise to an increase in CO_2 (electron acceptor) coverage and to a decrease in the coverage of H_2 (electron donor) [9–11,13,59].

In this way, depending on the relative electronegativity of the different adsorbates involved in the reaction and on which of them is in excess over the catalyst surface, the application of polarization will have a positive or negative effect on the overall kinetics of the process [9,59]. Namely, the electrochemical promotion allows modifying the adsorption of the different reactive molecules over the catalyst-electrode surface. Thus, there is a given value of potential or promoter coverage which optimizes catalyst activity and selectivity to the desired product, which depends on temperature and gas composition.

Therefore, the observed electrochemically assisted catalytic behaviour can be rationalized considering the effect of varying applied potential on the chemisorptive bond strength of reactants and intermediate surface species [9,59] and in accordance with the mechanisms proposed for the CO_2 hydrogenation reaction [44,47,50–52,60]. CO_2 can be chemisorbed and at least partly dissociated to CO on iron species (Fe and Fe_3O_4) on a clean Fe catalyst surface [44].

The pumping of O^{2-} species away from the catalyst surface to the solid electrolyte YSZ, enhances CO_2 (electron acceptor)

chemisorption (Eq. (9)) and dissociation to CO (Eq. (10). In fact, under application of negative potentials, a strengthening of the Fe-$(CO_2)^*$ bond strength is achieved [13], since O^{2-} species are pumped away from the catalyst surface to the solid electrolyte (YSZ), enhancing CO_2 adsorption and activation (Eq. (9)). Negative polarization also strengths Fe-C bond and weakens C—O bond enhancing CO_2 dissociation to CO (Eq. (10)).

The application of positive potentials give rise to a migration of oxygen ions to the catalyst surface, favouring H_2 (electron donor) dissociative adsorption (Eq. (20)) on Fe surface, resulting in an increase of the surface coverage of hydrogen and in a decrease in CO_2 coverage, being CO_2 (electron acceptor) adsorption the reaction limiting step.

$$H_2 \rightarrow 2H^{*+}(ads.) + 2e \triangle G^{\circ} = 38.9\,kJ\,mol^{-1} \quad (20)$$

At high O_2^- coverage or positive potentials, CO_2 dissociative adsorption on Fe is considered to be enhanced by the presence of coadsorbed hydrogen (Eq. (21)) [60].

According to literature [44,47,50–52,60], the mechanism of CO_2 hydrogenation on Fe based catalyst implies firstly CO_2 dissociative adsorption to adsorbed CO (Eqs. (10) or (21)) on the catalyst surface. CO adsorbed species resulting from CO_2 dissociation may desorb in the gas phase (Eq. (22)) or can react with H_2 to form CH_3OH (Eq. (23)), C_2H_6O (Eq. (24)) or CH_2 (Eq. (25)) adsorbed species. CH_2 adsorbed species are regarded as carbon–carbon propagation species with chain growth taking place, presumably, by addition of CH_2 units, resulting in the formation of hydrocarbons (mainly C_3H_6) (Eq. (26)). Subsequent hydrogenation of CH_2 species gives rise to adsorbed CH_3 species (Eq. (27)) which can be further hydrogenated to CH_4 (Eq. (28)) or can react with adsorbed CO to form CH_3CO adsorbed species (Eq. (29)) which subsequent hydrogenation results in ethanol formation (Eq. (30)) [60].

$$CO_2^{*-}(ads.) + e + 2H^+ \rightarrow CO^*(ads.) + H_2O \quad (21)$$

$$CO^*(ads.) \rightarrow CO \quad (22)$$

$$CO^*(ads.) + 4H(ads.) \rightarrow CH_3OH \quad (23)$$

$$3CO^*(ads.) + 6H(ads.) \rightarrow CH_3OCH_3 + CO_2 \quad (24)$$

$$CO^*(ads.) + 4H(ads.) \rightarrow CH_2^*(ads.) + H_2O \quad (25)$$

$$3CH_2^*(ads.) \rightarrow C_3H_6 \quad (26)$$

$$CH_2^*(ads.) + H(ads.) \rightarrow CH_3^*(ads.) \quad (27)$$

$$CH_3^*(ads.) + H(ads.) \rightarrow CH_4 \quad (28)$$

$$CH_2^*(ads.) + CO^*(ads.) + H(ads.) \rightarrow CH_3CO^*(ads.) \quad (29)$$

$$CH_3CO^*(ads.) + 3H(ads.) \rightarrow C_2H_5OH \quad (30)$$

At high positive potentials (hydrogen adsorption region), hydrogen coverage is supposed to be higher than that of CO adsorbed species resulting from CO_2 dissociation [13], and, thus, they can be gradually hydrogenated to C_2H_6O and C_2H_5OH.

It can be observed that under application of decreasing positive potentials to negative values (up to about −0.5 V), a migration of oxygen ions from the catalyst surface to the solid electrolyte is produced, decreasing oxygen surface coverage [9]. As a result, the adsorption of electron acceptor species, as CO_2 (Eq. (9)), is favoured [59] due to its higher electronegativity [61], increasing their surface coverage at the expense of electron donors (hydrogen) and giving rise to a progressive increase in surface CO formation by dissociative adsorption of CO_2, whereas H_2 (electron donor) dissociative adsorption on Fe is hindered and therefore hydrogen evolution is favoured [5,13]. As a result, CO selectivity increases and selectivity to C_2H_6O and C_2H_5OH decreases on decreasing catalyst potential [13].

In fact, on decreasing applied potential, a strengthening of the Fe-$(CO_2)^*$ bond strength is achieved [13], since O^{2-} species are pumped away from the catalyst surface to the solid electrolyte (YSZ), enhancing CO_2 adsorption and activation (Eq. (9)), whereas H_2 dissociative adsorption (Eq. (20)) on Fe surface is hindered. Lowering applied potentials also strengths Fe-C bond and weakens C—O bond enhancing CO_2 dissociation to CO (10), resulting in an enhancement of CO formation [10,11,13]. Moreover, CO dissociative adsorption is less favoured at lower potentials (CO has a lower electron acceptor capacity than CO_2) [9,11,59,62] and it tends to desorb (Eq. (22)). Both phenomena result in an increase in the selectivity to CO.

Moreover, it can be observed that under application of decreasing positive potentials formation of CH_3OH is increasingly enhanced reaching a maximum at about −0.5 V. As commented above, around open circuit conditions (−0.5 V), at low negative or positive potentials, selectivity to CH_3OH exhibited a maximum, showing a "volcano type" electrochemical behaviour. In fact, formation of CH_3OH is reported to be enhanced over almost promoter free metal surfaces (around 0 V), where surface coverage of both reactants (CO_2 and H_2) is expected to be very similar. Therefore, a strong competition between CO_2 and H_2 adsorption could be expected within this potential range, and, thus, according to this mechanism, it is expected that the formation of CH_3OH will be limited by the dissociative adsorption of both H_2 and CO_2 [63,64].

A subsequent decrease in potential below −0.5 V, gives rise to an enhancement of CO_2 dissociative adsorption on Fe surface, via formation of adsorbed CO species, and to a decrease in H_2 dissociative adsorption, because H_2 adsorption is retarded and tends to be evolved from the catalyst surface [5,13]. Therefore, the amount of hydrogen adsorbed on the surface is reduced and could limit CO_2 hydrogenation reactions. CO selectivity increases on decreasing applied potential, because CO formation (via enhanced CO_2 dissociative adsorption) and desorption (given that CO has a lower electron acceptor capacity than CO_2) are favoured. As commented above, selectivity to C_2H_5OH selectivity exhibited a concomitant minimum at the same potential value (−0.5 V) as selectivity to CH_3OH exhibited a maximum, resembling an "inverted volcano type" electrochemical behaviour. Therefore, selectivity to C_2H_5OH increases on decreasing applied potential below −0.5 V due to the enhanced adsorbed CO, and thus CH_3CO^*, species formation, as a result of the improved CO_2 dissociation via O^{2-} abstraction, because, in spite of hydrogen evolution (which may limit the CO_2 hydrogenation) is also favoured on decreasing applied potential, under a stoichiometric H_2/CO_2 ratio of 3, hydrogen coverage is still enough [13] for CH_3CO^* adsorbed species to be hydrogenated to C_2H_5OH, given that CH_3OH formation is inhibited (sharply decrease to almost zero) for negative potentials [63]. As a consequence, C_2H_5OH formation competitive reaction is increasingly enhanced, resulting in an increase in C_2H_5OH selectivity, with the decrease in potential. On the contrary, selectivity to C_2H_6O decreases for potentials below −0.5, because, as commented above, the coverage of both hydrogen and CO adsorbed species decreases on lowering applied potential resulting in a decrease in selectivity to C_2H_6O [2,12,13].

The steady state response of CO_2 conversion, Turn Over Frequency (TOF) and CO_2 rate enhancement ratio to different applied catalyst potentials (between −1.5 and 1.5 V), at 325 °C and 90 l h^{-1} and using a H_2/CO_2 ratio of 4, is displayed in Fig. 5a. Fig. 5b shows the effect of applied potential on the selectivity to CO, CH_3OH, C_2H_6O, C_2H_5OH and C_3H_6, respectively, whereas Fig. 5c shows the variation of apparent faradaic efficiency ($|\Lambda|$) and current with applied potential, under the same conditions.

As can be observed in Fig. 5b, for H_2/CO_2 ratios of 4, the hydrogenation of CO_2 over Fe-TiO_2/YSZ/Au, at 325 °C and 90 l h^{-1}, gives rise also to the formation of CO (Eq. (2)), CH_3OH (Eq. (13)), C_2H_6O

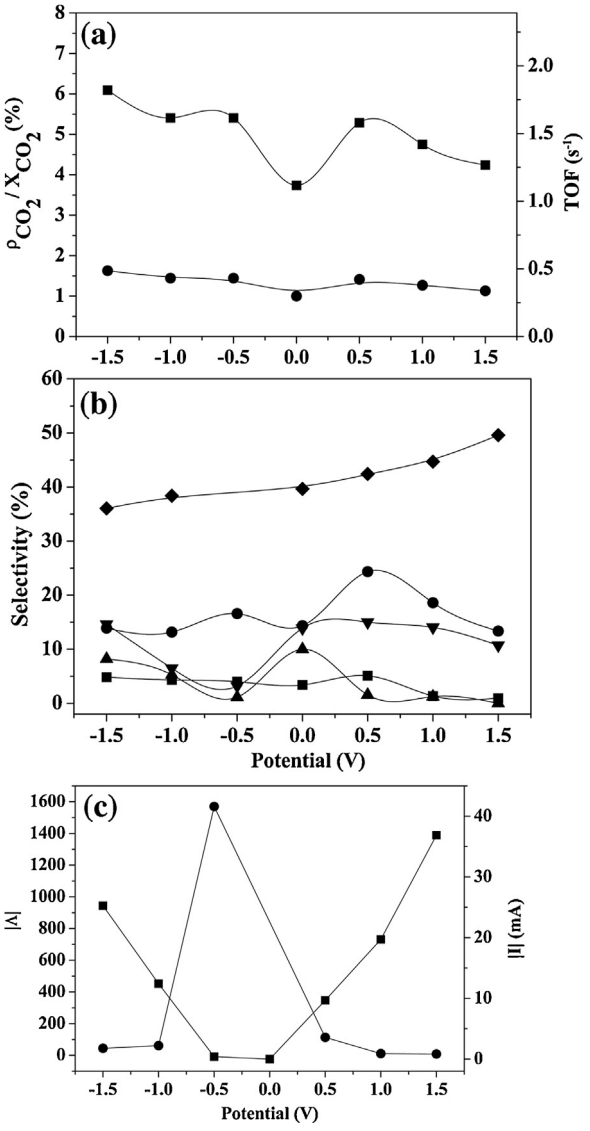

Fig. 5. Influence of the applied potential on (a) CO_2 conversion/TOF (■) and CO_2 rate enhancement ratio (●), on (b) selectivities to CH_3OH (■), C_2H_6O (●), CO (▲), C_2H_5OH (▼) and C_3H_6 (♦) and on (c) current (■) and apparent faradaic efficiency (●) over Fe-TiO_2/YSZ/Au. (325 °C, 90 l h^{-1}, H_2/CO_2 = 4).

(Eq. (14)), C_2H_5OH (Eq. (17)) and C_3H_6 (Eq. (31)), and it is, as well, affected by the applied potential, with selectivities to CO, CH_3OH, C_2H_6O, C_2H_5OH and C_3H_6 up to about 10%, 5%, 25%, 15% and 50%, respectively.

$$3CO_2 + 9H_2 \rightarrow C_3H_6 + 6H_2O \triangle G^\circ = -177\,kJ\,mol^{-1} \quad (31)$$

CO_2 rate enhancement ratio values are again rather low (up to about 1.6) with CO_2 conversions up to 6% and TOF up to 1.7 s^{-1}. The catalyst resembled, as well, an "inverted volcano type" electrochemical behaviour, showing also a minimum in CO_2 rate enhancement ratio at about 0 V (Fig. 5a) [9,59].

As can be observed in Fig. 5c, $|\Lambda| > 1$ for whatever value of applied potential. The maximum value of $|\Lambda|$ is obtained for −0.5 V and resulted to be 1570, demonstrating the non-Faradaic nature of the process [9].

For this high H_2/CO_2 ratio, the performance of the catalyst is similar to that obtained for a H_2/CO_2 ratio of 3, but the main product obtained is C_3H_6. Therefore, the selectivity to C_3H_6 has been also plotted consequently.

C_3H_6 is reported to be formed from CH_2 radicals (Eq. (26)) resulting from hydrogenation of CO adsorbed species deposited by CO_2 dissociation. The increase in the formation of C_3H_6 is thought to be due to the presence of an excess of H_2 with respect to that stochiometrically required for CH_3OH and C_2H_6O formation (H_2/CO_2 ratio of 3), i.e., due to an increased H_2 availability in the system. In fact according to literature [47,49], higher hydrocarbon selectivity is attributable to a hydrogen excess in the reaction system [47,49].

Selectivity to C_3H_6 diminished with potential decrease (Fig. 5b), i.e., an electrophobic electrochemical behaviour is observed, because, as commented above, on decreasing applied potential, H_2 (electron donor) dissociative adsorption is hindered and hydrogen evolution is favoured [5,13], limiting adsorbed CO species hydrogenation to CH_2, and thus, C_3H_6 formation. In addition, as more water is formed, the amount of surface CO generated by CO_2 dissociation could decrease also trough the WGS (water gas shift) (Eq. (32)) [65], resulting in a concomitant decrease in C_3H_6 yield.

$$CO + H_2O \rightarrow CO_2 + H_2 \triangle G^\circ = -19.9\,kJ\,mol^{-1} \quad (32)$$

Moreover, it can be observed that under application of decreasing positive potentials within the positive range, formation of CH_3OH and C_2H_6O is increasingly promoted reaching a maximum at about 0.5 V. As indicated above, under application of high positive potentials, H_2 (electron donor) dissociative adsorption on Fe surface is favoured, being CO_2 (electron acceptor) adsorption the reaction limiting step. CO_2 dissociation is considered to be enhanced by the presence of adsorbed hydrogen. Hydrogenation of CO adsorbed species resulting from CO_2 dissociation leads to the formation of these oxygenated products. Decreasing catalyst potential results in the migration of oxygen species to the solid electrolyte favouring CO_2 (electron acceptor) dissociate adsorption on Fe surface, whereas H_2 dissociative adsorption is hindered. As a result, selectivity to CH_3OH and C_2H_6O increases up to a maximum value, which corresponds with a maximum enhancement in its selectivity of up to 50 and 1.7 times, respectively. In this case, selectivities to CH_3OH and C_2H_6O showed similar trends against potential, because in spite of hydrogen dissociative adsorption is hindered on decreasing applied potentials, for H_2/CO_2 ratios of 4 (higher than the stoichiometric ratio) hydrogen coverage is always higher than that of CO adsorbed species resulting from CO_2 dissociation [56] and thus CO adsorbed species can be gradually hydrogenated to both compounds. Therefore, the competition between hydrogenation reactions is less pronounced. A subsequent decrease in potential results in a decrease in selectivity to CH_3OH and C_2H_6O, because the hydrogen evolution reaction is increasingly favoured, and the amount of hydrogen adsorbed on the surface is reduced limiting hydrogenation reactions.

In general, the variation of C_2H_5OH and CO selectivities vs. applied potential is very similar to that observed for a H_2/CO_2 ratio of 3.

In this case the maximum in C_3H_6 and C_2H_5OH formation corresponds with an enhancement in their selectivity of up to about 1.4 and 150 times, respectively, whereas the concomitant minimum in CO formation corresponds with a decrease in its selectivity of up to approximately 100 times.

Fig. 6 shows the steady state effect of the applied potential on CO_2 conversion, Turn Over Frequency (TOF) and CO_2 rate enhancement ratio (Fig. 6a) and on the selectivity to CO, CH_3OH, C_2H_6O and C_2H_5OH (Fig. 6b), respectively, at 325 °C and 90 l h^{-1} and using a H_2/CO_2 ratio of 2, whereas Fig. 6c shows the variation of apparent faradaic efficiency ($|\Lambda|$) and current with applied potential, under the same conditions.

As can be observed in Fig. 6b, for H_2/CO_2 ratios of 2, the hydrogenation of CO_2 over Fe-TiO_2/YSZ/Au, at 325 °C and 90 l h^{-1}, gives rise to the formation of CO (Eq. (2)), CH_3OH (Eq. (13)), C_2H_6O (Eq. (14)) and C_2H_5OH (Eq. (17)), being a competition for the formation

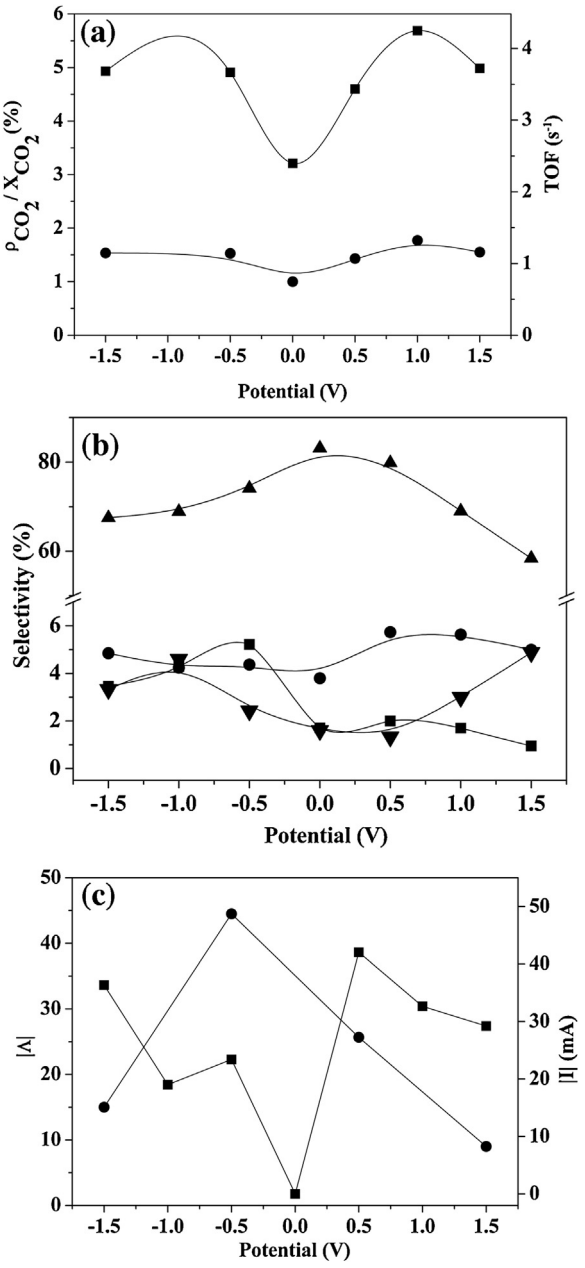

Fig. 6. Influence of the applied potential on (a) CO_2 conversion/TOF (■) and CO_2 rate enhancement ratio (●), on (b) selectivities to CH_3OH (■), C_2H_6O (●), CO (▲) and C_2H_5OH (▼) and on (c) current (■) and apparent faradaic efficiency (●) over Fe-TiO_2/YSZ/Au. (325 °C, 90 l h^{-1}, H_2/CO_2 = 2).

of the different hydrogenation products over the catalyst surface, and it is, as well, perceptibly influenced by the applied potential, with selectivities to CO, CH_3OH, C_2H_6O and C_2H_5OH up to about 80%, 6%, 5% and 5%, respectively.

CO_2 rate enhancement ratio values are rather low (up to about 1.5). CO_2 conversion is also fairly low (up to 5%) with TOF values up to 4.2. The catalyst showed also an "inverted volcano type" electrochemical behaviour, i.e., CO_2 rate enhancement ratio exhibits a minimum at a certain potential (under open circuit conditions approx.) (Fig. 6a) [8,59].

As can be observed in Fig. 6c, $|\Lambda| > 1$ for whatever value of applied potential. The maximum value of $|\Lambda|$ is obtained for −0.5 V and resulted to be 44.5, demonstrating the non-Faradaic character of the process [9].

For this lower H_2/CO_2 ratio, the electrochemical behaviour is similar to that obtained for an H_2/CO_2 ratio of three, but CO is produced dominantly for all range of potentials, due to the defect of H_2 [49] with respect to that required by stoichiometry for methanol and dimethyl ether formation (H_2/CO_2 ratio of 3) and closer to that required for reverse water gas shift reaction (H_2/CO_2 ratio of 1).

Under high positive potentials H_2 adsorption is favoured, being CO_2 adsorption the reaction limiting step. In this case, on decreasing catalyst potential CO selectivity increases and selectivity to C_2H_6O and C_2H_5OH decreases due to the improved CO formation (via CO_2 dissociation) and desorption (CO has a lower electron donor capacity than H_2), and enhanced hydrogen evolution on decreasing potential. For H_2/CO_2 ratios of 2 (lower than the stoichiometric ratio for C_2H_6O and C_2H_5OH formation) and on hydrogen adsorption region (positive potential) coverage of H_2 is still higher enough for CO adsorbed species to be partially hydrogenated. On hydrogen evolution region (negative potential), H_2 coverage is lower, in addition CO formation and desorption (CO has a lower electron acceptor capacity than CO_2) are favoured as a result of the enhanced CO_2 dissociative adsorption, being RWGS the dominant reaction. However, as more water is formed from CO_2 hydrogenation reactions, the amount of CO could decrease also through the WGS (water gas shift) (Eq. (32)) reaction [65], resulting in a concomitant decrease in CO yield, giving rise to the observed decrease in CO selectivity and providing surface CO_2 and H_2 adsorbed species needed for the different oxygenates production.

In this case, selectivity to CH_3OH, C_2H_6O and C_2H_5OH showed the same tendency vs. applied potential variation as for an H_2/CO_2 ratio of 3, showing a "volcano type" (maximum at −0.5 V), "electrophobic" and "inverted volcano type" (minimum at 0 V) electrochemical behaviour, respectively, whereas CO selectivity exhibited also a "volcano type" electrochemical behaviour, i.e. it attained also a maximum at a given potential value (0 V).

In fact, as shown in Fig. 6b, with increasing catalyst potential by approximately 0.5 V (from 0 to 0.5 V), the selectivity to C_2H_6O increases by 1.5 times. As can be also observed in Fig. 6b, with increasing catalyst potential by about 1.5 V (from 0 to 1.5 V), C_2H_5OH selectivity increases by about 12.5 times and CO selectivity decreases by about 1.3 times.

As can be deduced also from Fig. 6b, the optimum applied potential for CH_3OH formation is about −0.5 V, which corresponds with an enhancement in their selectivity of up to about 2.5 times (with respect to unpromoted open circuit conditions).

One of the main challenges for advancing CO_2 hydrogenation to fuels is increasing the energy efficiency of the process, i.e., decreasing the energy requirements for producing the products. The trend is to maximize products yield with minimal energy input. However, as stated in the introduction part of the manuscript, there are other aspects which may justify the application of the electropromoted CO_2 hydrogenation to fuels even with low energy efficiency, because this technology offers a way for chemical storage of the surplus of intermittent renewable energy that would otherwise be wasted, turning the excess electricity, through electrolysis of water, into renewable hydrogen which can be used to produce fuels.

From the above commented results, it seems that the control of the yield of the CH_3OH, C_2H_5OH and C_2H_6O can be carried out by modification of the applied potential, i.e., there is an optimum value of potential, at a given flow rate, temperature and H_2/CO_2 and ratio, which maximized CH_3OH, C_2H_5OH or C_2H_6O selectivity.

The energy efficiency (energy balance) of the overall process can be calculated as the ratio between useful energy that can be produced by combustion of the synthesised fuel (output energy) and the energy consumed in the formation of the product. The energy produced can be calculated by multiplying the amount of fuel produced by its calorific value, whereas the consumed energy can be calculated as the sum of the thermal energy (needed to

increase temperature of reactives to that required for the reaction) and electrical energy (needed to supply the current needed for electropromotion of the process) necessary for obtaining the fuel product. Therefore, the energy efficiency (energy balance) of the overall process should be calculated for each target product formation.

The electrical energy requirements for producing the different products can be evaluated from the values of energy cost (kWh/Kg) associated with each product formation calculated according to Eq. (8). In this work, the energy cost (kWh/Kg) has been calculated for each product fuel (methanol, ethanol and dimethyl ether) formation under different operating conditions as an indication of the energy efficiency of the process.

The minimum value of energy cost (kWh/Kg) associated with each product formation was 0.004, 0.003 and 0.0005, for methanol, ethanol and dimethyl ether, respectively. These values were obtained for −0.5 V at 325 °C and using H_2/CO_2 ratios of 3 (for methanol and ethanol) and 4 (for C_2H_6O). In the case of methanol, the minimum in energy cost coincides with the maximum in CH_3OH selectivity, which makes methanol a candidate target product, but also with a rather low CO_2 conversion and high selectivity to the rest of the products, which implies an additional cost associated with product purification.

3.2.3. *Effect of H_2/CO_2 ratio*

For better understanding of the influence of H_2/CO_2 ratio on catalyst behaviour and selectivity to the different products, the potentiostatic variation of CO_2 conversion, CO_2 rate enhancement ratio and selectivity to CO, CH_3OH, C_2H_5OH, and C_2H_6O are plotted for different H_2/CO_2 ratios in Fig. 7a–f, respectively.

Results (Fig. 7a) indicate that, in general, CO_2 conversion is slightly affected by H_2/CO_2 ratio, except in the case of H_2/CO_2 ratio of three where the CO_2 conversion versus potential curve is shifted to the highest values of conversion, in special at highly negative potentials.

As can be deduced from Fig. 7b, at positive potentials, in general, CO_2 rate enhancement ratios, i.e., promotion levels, decrease on increasing H_2/CO_2 ratio.

Selectivity to CO increases on decreasing H_2/CO_2 ratio, as result of the decreased hydrogen availability with respect to the stoichiometrically required for the synthesis of the different hydrogenated products. In the case of H_2/CO_2 ratio of two, the CO selectivity vs. potential curve is shifted to the highest values (between 60 and 80%), presumably because an H_2/CO_2 ratio of two is closer to the value required by stoichiometry for RWGS reaction (about 1), favouring CO production.

CH_3OH selectivity (Fig. 7d) exhibits a maximum around open circuit conditions (+0.5–0.5 V), because the surface reaction could be restricted by the coverage of both CO_2 and H_2 adsorbed on the catalyst surface [63,64], and for H_2/CO_2 ratios equal to three (of about 50%), which corresponds with that required for stoichiometric synthesis of methanol by CO_2 hydrogenation (Eq. (10)), and, therefore, thermodynamically favours the formation of CH_3OH as the expenses of other CO_2 hydrogenation products. On the other hand, for H_2/CO_2 ratios distinct from three, selectivity to methanol was almost unaffected by H_2/CO_2 ratio [66].

Selectivity to ethanol (Fig. 7e) follows an opposite trend vs. H_2/CO_2 ratio with respect to methanol selectivity, showing a minimum at about −0.5 V, which seems to indicate that they are formed through competitive reactions. For other potential values, selectivity to ethanol increases with H_2/CO_2 ratio [67], as result of the increased hydrogen availability with respect to the stoichiometrically required for the ethanol synthesis reaction.

As can be obtained from Fig. 7f, for an H_2/CO_2 ratio of three, the C_2H_6O selectivity vs. potential curve is shifted to the highest values (between 25 and 50%), presumably because this H_2/CO_2 ratio coin-

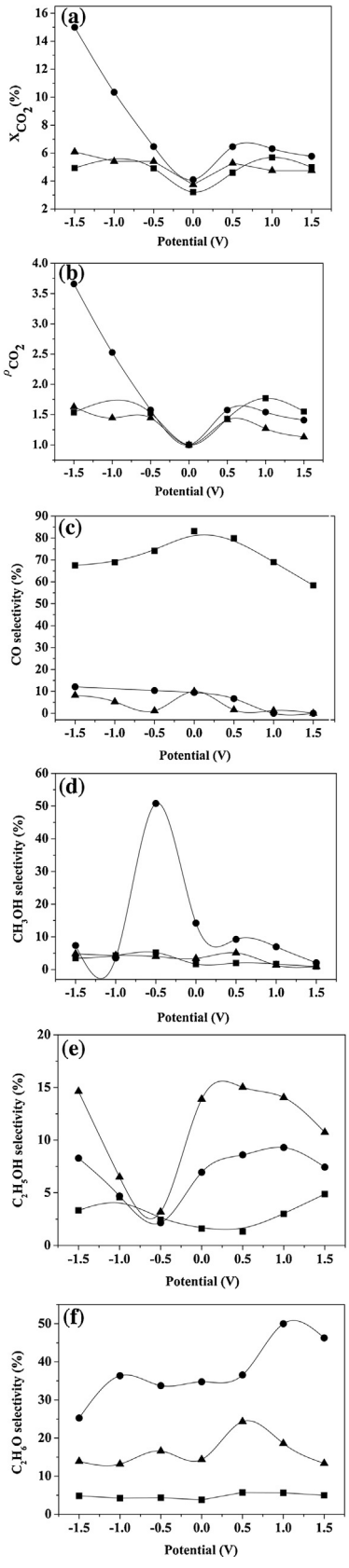

Fig. 7. Effect of H_2/CO_2 ratio on the potentiostatic variation of CO_2 conversion (a), CO_2 rate enhancement ratio (b) and selectivities to CO (c), CH_3OH (d), C_2H_5OH (e) and C_2H_6O (f) on Fe-TiO_2/YSZ/Au. (325 °C, H_2/CO_2 = 2 (■), H_2/CO_2 = 3 (●) and H_2/CO_2 = 4 (▲), 90 l h^{-1}).

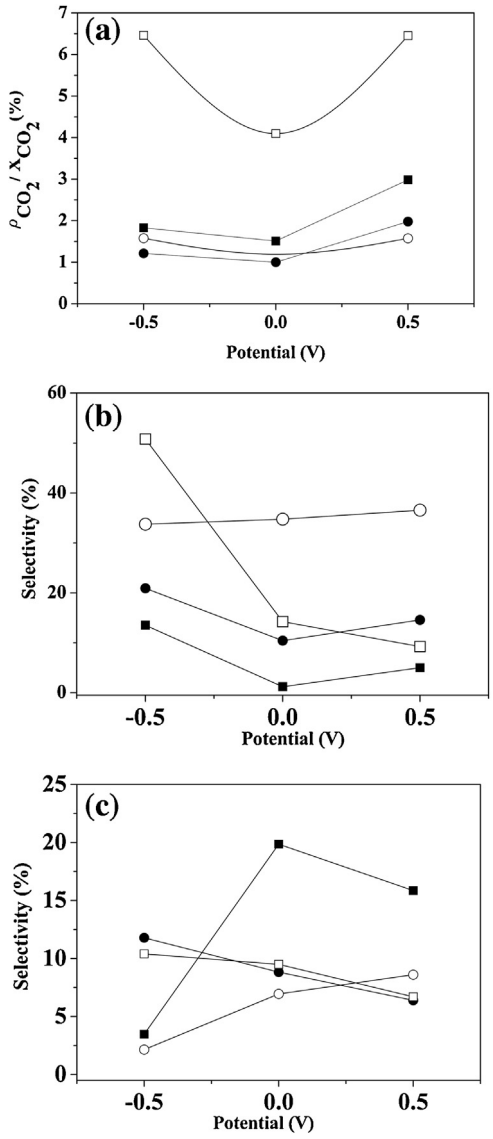

Fig. 8. Effect of gas flow rate on the potentiostatic variation of (a) CO_2 conversion (■,□) and CO_2 rate enhancement ratio (●,○), (b) selectivity to CH_3OH (■,□) and C_2H_6O (●,○) and (c) selectivity to CO (■,□) and C_2H_5OH (●,○) at 216 l h^{-1} (filled symbols) and 90 l h^{-1} (open symbols) over Fe-TiO_2/YSZ/Au. (325 °C, H_2/CO_2 = 3).

cides with that required for stoichiometric synthesis of C_2H_6O by CO_2 hydrogenation (Eq. (14)), and, therefore, thermodynamically favours the formation of C_2H_6O as the expenses of other CO_2 hydrogenation products. On the other hand, for H_2/CO_2 ratios distinct from three, selectivity to dimethyl ether decreased on increasing H_2/CO_2 ratio.

As commented above, selectivity to C_3H_6 reaches a maximum for a H_2/CO_2 ratio of 4, because the amount of hydrogen is in excess with respect to that required by stoichiometry for the synthesis reactions via CO_2 hydrogenation [47].

3.2.4. *Effect of gas flow rate*

The influence of gas flow rate (the reciprocal of contact time) on CO_2 hydrogenation behaviour, at 325 °C and using a H_2/CO_2 ratio of 3, is depicted in Fig. 8. Results indicate that increasing gas flowrate, and correspondingly, decreasing contact time, resulted in a decrease in CO_2 conversion (Fig. 8a) and in CH_3OH and dimethyl ether selectivities (Fig. 8b), as well as in an increase in CO and C_2H_5OH selectivities (Fig. 8c), whereas CO_2 rate enhancement ratio is almost unaffected by the variation of gas flow rate (Fig. 8a).

As expected, the CO_2 conversion values decreased upon increasing gas flow rate as a result of the lower contact time available for the reaction to take place, and, very interestingly, the methanol and dimethyl ether selectivity also followed a negative trend [68,69]. This seems to suggest that both CH_3OH and C_2H_6O were produced, to a large extent, from the CO hydrogenation, as a consecutive step of the RWGS reaction, rather from the direct CO_2 hydrogenation reaction. On the contrary, selectivity to C_2H_5OH and CO increases on increasing gas flow rate. This could be indicative of the fact that C_2H_5OH and CO are produced in parallel paths through the corresponding hydrogenation reactions, because a diminution in selectivity to C_2H_5OH with the increase in gas flow rate could be expected if C_2H_5OH was produced via consecutive hydration or hydrogenation of the formed CH_3OH [70,71]. However, C_2H_6O selectivity decreases with the increment in gas flowrate as CH_3OH does, which seems to indicate that C_2H_6O is formed in any consecutive reaction from CH_3OH (via consecutive dehydration of the formed CH_3OH) or from the same reaction intermediate (CO) [70,71].

The observed decrease in C_2H_5OH selectivity at higher residence times could resemble a possible inhibition of primary ethanol synthesis, via hydrogenation of the adsorbed CO deposited by CO_2 dissociation, by H_2O formed as side product of higher alcohols and by hydrocarbons secondary reactions of adsorbed CO with CH_2^* radicals, which are favoured by long residence times [51,69].

4. Conclusions

In this study, a Fe-TiO_2/YSZ/Au tubular electrochemical catalyst has been successfully prepared by dip-coating and characterised, both after reduction and after testing, by Scanning Electron Microscopy, X-Ray Photoelectron Spectroscopy and X-Ray Diffraction techniques.

The CO_2 hydrogenation over Fe in an oxygen ion conducting membrane reactor can be electrochemically assisted under atmospheric pressure, at relatively low temperatures and high gas flow rates and under realistic postcombustion CO_2 capture exiting gas compositions. Selectivity to the different target fuels can be modulated by modifying applied potential under given operating conditions.

The hydrogenation of CO_2 over the Fe catalyst leads to different products depending on operating conditions. The main products were methanol, dimethyl ether, ethanol, CO and C_3H_6, but CH_4, C_2H_6, formic acid and acetic acid were also detected to be formed.

CO_2 hydrogenation and selectivities to CH_3OH, C_2H_6O, C_3H_6 and C_2H_5OH were electrochemically enhanced up to a maximum of 50, 1.7, 1.4 and 150 times, respectively.

A temperature value of 325 °C was selected to be the optimum for the electrochemically assisted CO_2 hydrogenation process.

Increasing gas flow rate, and correspondingly, decreasing contact time, for a given H_2/CO_2 ratio of 3 and at 325 °C, resulted in a decrease in CO_2 conversion and in CH_3OH and dimethyl ether selectivities and in an increase in CO and C_2H_5OH selectivities, whereas CO_2 rate enhancement ratio is almost unaffected by the variation of gas flow rate.

Results obtained at different H_2/CO_2 ratios, at 90 l h^{-1} and 325 °C, showed that CO_2 conversion and selectivities to CH_3OH and C_2H_6O showed a maximum for a H_2/CO_2 ratio of 3, whereas selectivites to C_3H_6 and CO strongly increase for a H_2/CO_2 ratio of 4 and 2, respectively, as a result of the increased and decreased hydrogen availability in the reaction system, and selectivity to C_2H_5OH increases with the increment in H_2/CO_2 ratio, being the maximum values attained around 80%, 50%, 50%, 15% and 47% for CO, C_3H_6, CH_3OH, C_2H_5OH and C_2H_6O, respectively.

Therefore, this study addresses some scale-up aspects, such as operation at high flow rates and atmospheric pressure, under realistic gas compositions and using catalyst-electrode configurations easily adaptable to the existing catalytic devices (conventional flow reactors), based on a cheap, widespread and non-precious Fe catalyst, and prepared by commercial ready procedures, which may have an impact on the potential practical application of the process for CO_2 recycling, contributing not only to controlling the global "Green-house Effect", but also to the availability of fuel sources for the future.

Acknowledgements

The authors acknowledge support from Ministerio de Ciencia e Innovación of Spain (Project ENE2010-15569). Pedro J. Martinez is grateful to Ministerio de Ciencia e Innovación of Spain for the research grant BES-2011-046902.

Appendix A. Supplementary data

Supplementary data associated with this article can be found, in the online version, at http://dx.doi.org/10.1016/j.cattod.2016.02.025.

References

[1] G.A. Olah, A. Goeppert, G.K.S. Prakash, J. Org. Chem. 74 (2009) 487–498.
[2] F. Ocampo, B. Louis, A. Kiennemann, A.C. Roger, Mater. Sci. Eng. 19 (2011) 1–11.
[3] S.K. Hoekman, A. Broch, C. Robbins, R. Purcell, Int. J. Greenh. Gas Control 4 (2010) 44–50.
[4] D.T. Whipple, P.J. Kenis, J. Phys. Chem. Lett. (2010) 3451–3458.
[5] E.I. Papaioannou, S. Souentie, A. Hammad, C.G. Vayenas, Catal. Today 146 (2009) 336–344.
[6] W. Wang, S. Wang, X. Ma, J. Gong, Chem. Soc. Rev. 40 (2011) 3703–3727.
[7] A. Anastasijevic, Catal. Today 146 (2009) 308–311.
[8] G. Karagiannakis, S. Zisekas, M. Stoukides, Solid State Ionics 162–163 (2003) 313–318.
[9] C.G. Vayenas, S. Bebelis, C. Pliangos, S. Brosda, D. Tsiplakides, Electrochemical Activation of Catalysis: Promotion Electrochemical Promotion and Metal-Support Interactions, Kluwer Academic/Plenum Publishers, New York, 2001.
[10] G. Pekridis, K. Kalimeri, N. Kaklidis, E. Vakouftsi, E.F. Iliopoulou, C. Athanasiou, G.E. Marnellos, Catal. Today 127 (2007) 337–346.
[11] S. Bebelis, H. Karisali, C.G. Vayenas, Solid State Ionic 179 (2008) 139–1395.
[12] S. Bebelis, H. Karasali, C.G. Vayenas, J. Appl. Electrochem. 38 (2008) 1127–1133.
[13] D. Theleritis, S. Souentie, A. Siokou, A. Katsaounis, C.G. Vayenas, ACS Catal. 2 (2012) 770–780.
[14] D. Theleritis, M. Makri, S. Souentie, A. Caravaca, A. Katsaounis, C.G. Vayenas, ChemElectroChem 1 (2014) 254–262.
[15] M. Makri, A. Katsaounis, C.G. Vayenas, Electrochim. Acta 179 (2015) 556–564.
[16] I. Kalaitzidou, A. Katsaounis, T. Norby, C.G. Vayenas, J. Catal. 331 (2015) 98–109.
[17] I. Kalaitzidou, M. Makri, D. Theleritis, A. Katsaounis, C.G. Vayenas, Surf. Sci. 646 (2016) 194–203.
[18] V. Jiménez, C. Jiménez-Borja, P. Sánchez, A. Romero, E.I. Papaioannou, D. Theleritis, S. Souentie, S. Brosda, J.L. Valverde, Appl. Catal. B 107 (2011) 210–220.
[19] N. Gutiérrez-Guerra, J. González-Cobos, J.C. Serrano-Ruiz, J.L. Valverde, A. de Lucas-Consuegra, Top. Catal. (2015), http://dx.doi.org/10.1007/s11244-015-0488-4 (published online).
[20] D. Tsiplakides, S. Balomenou, Chem. Ind. Chem. Eng. Q. 14 (2008) 97–105.
[21] D. Tsiplakides, S. Balomenou, Catal. Today 146 (2009) 312–318.
[22] E. Ruiz, D. Cillero, P.J. Martínez, A. Morales, G. San Vicente, G. de Diego, J.M. Sánchez, Catal. Today 210 (2013) 55–66.
[23] E. Ruiz, D. Cillero, P.J. Martínez, A. Morales, G. San Vicente, G. de Diego, J.M. Sánchez, Catal. Today 236 (2014) 108–120.
[24] E. Ruiz, D. Cillero, P.J. Martínez, A. Morales, G. San Vicente, G. de Diego, J.M. Sánchez, J. CO_2 Util. 8 (2014) 1–20.
[25] P.R. Strutt, B.H. Kear, US Patent 8,173,327 B2.
[26] D. Poulidi, A. Thursfield, I.S. Metcalfe, Top. Catal. 44 (2007) 435–449.
[27] A. Morales, EU EP 1 321 539 A2.
[28] C. Pliangos, I.V. Yentekakis, S. Ladas, C.G. Vayenas, J. Catal. 159 (1996) 189–203.
[29] E.A. Baranova, G. Foti, H. Jotterand, C. Comninellis, Top. Catal. 44 (2007) 355–360.
[30] W. Wang, J. Gong, Front. Chem. Sci. Eng. 5 (2011) 2–10.
[31] C. Guizard, A. Princivalle, Catal. Today 146 (2009) 367–377.
[32] E. Mutoro, C. Koutsodontis, B. Luerssen, S. Brosda, C.G. Vayenas, J. Janek, Appl. Catal. B 100 (2010) 328–337.
[33] Y.-x Pan, C.-j. Ge, T.S. Liu, Q. Ge, Catal. Today 147 (2009) 68–76.
[34] J.-S. Kim, S.-B. Lee, M.-J. Choi, K.-W. Lee, Catal. Today 115 (2006) 228–234.
[35] M. Kisida, K. Umakoshi, J. -i. Ishiyama, H. Nagata, K. Wakabayashi, Catal. Today 29 (1996) 355–359.
[36] A. de Lucas Consuegra, A. Caravaca, J. Gonzalez-Cobos, J.L. Valverde, F. Dorado, Catal. Commun. 15 (2011) 6–9.
[37] C.S. Chen, J.H. You, J.H. Lin, Y.Y. Chen, Catal. Commun. 9 (2008) 2381–2385.
[38] X. Yao, Q. Yu, Z. Ji, Y. Lu, Y. Cao, C. Tang, F. Gao, L. Dong, Y. Chen, Appl. Catal. B 130–131 (2013) 293–304.
[39] C.H. Bartholomew, R.J. Farrauto, Fundamentals of Industrial Catalytic Processes, 2nd ed., John Wiley & Sons, Inc, New Jersey, 2006.
[40] Z. Shu, S. Wang, J. Nanomater. 2009 (2009) 340217, http://dx.doi.org/10.1115/2009/340217.
[41] K. Cheng, V.V. Ordomsky, M. Virginie, B. Legras, P.A. Chernavskii, V.O. Kazak, C. Cordier, S. Paul, Y. Wang, A.Y. Khodakov, Appl. Catal. A 488 (2014) 66–77.
[42] R.W. Dorner, D.R. Hardy, F.W. Williams, H.D. Willauer, Appl. Catal. A 373 (2010) 112–121.
[43] T. Yamashita, P. Hayes, Appl. Surf. Sci. 254 (2008) 2441–2449.
[44] M. Niemelä, M. Nokosmaki, Catal. Today 100 (2005) 269–274.
[45] J.S. Hwang, K.W. Jun, K.W. Lee, Appl. Catal. A 208 (2001) 217–222.
[46] Z.L. Liu, H.B. Wang, Q.H. Lu, G.H. Du, L. Peng, Y.Q. Du, S.M. Zhang, K.L. Yao, J. Magn. Magn. Mater. 283 (2004) 258–262.
[47] S. Seidi, N.A.S. Amin, M.R. Rahimpour, J. CO_2 Util. 5 (2014) 66–81.
[48] T. Inui, M. Anpo, K. Izui, S. Yanegida, T. Yamaguchi, Advanced in Chemical Conversions for Mitigating Carbon Dioxide, Elsevier Science B V, Amsterdam, 1998.
[49] S. Zhanghuai, K. Yuan, J. Nat. Gas Chem. 9 (2000) 283–290.
[50] H.D. Willauer, R. Ananth, M.T. Olsen, D.M. Drab, D.R. Hardy, F.W. Williams, J. CO_2 Util. 3–4 (2013) 56–64.
[51] D. Miller, M. Moskovits, J. Am. Chem. Soc. 111 (1989) 9250–9252.
[52] C.M. Finnerty, N.J. Coe, R.H. Cunningham, R.M. Ormerod, Catal. Today 46 (1998) 137–145.
[53] H. Schulz, T. Riedel, G. Schaub, Top. Catal. 32 (2005) 117–124.
[54] S.J. Choe, D.H. Park, D.S. Huh, Bull. Korean Chem. Soc. 21 (2000) 779–784.
[55] C. Schild, A. Wokaun, R.A. Koeppel, A. Baiker, J. Phys. Chem. 95 (1991) 6341–6346.
[56] R. Sahki, O. Benlounes, O. Chérifi, R. Thouvenot, M.M. Bettahar, S. Hocine, React. Kinet. Mech. Catal. 103 (2011) 391–403.
[57] Y. Souma, H. Ando, M. Fujiwara, R. Kieffer, Energy Convers. Manag. 36 (1995) 593–596.
[58] S. Li, A. Li, S. Krishnamoorthy, E. Iglesia, Catal. Lett. 77 (2001) 197–205.
[59] S. Brosda, C.G. Vayenas, J. Wei, Appl. Catal. B 68 (2006) 109–124.
[60] H. Kusama, K. Okabe, K. Sayama, H. Arakawa, Energy 22 (1997) 343–348.
[61] F.J. Willians, M.S. Tikhov, A. Palermo, N. Macleod, R.M. Lambert, J. Phys. Chem. B 105 (2001) 2800–2808.
[62] M. Kuriyama, H. Tanaka, S. Ito, T. Kubota, T. Miyao, S. Naito, K. Tomishige, K. Kunimori, J. Catal. 252 (2007) 39–48.
[63] P. Dube, G.M. Brisard, J. Electroanal. Chem. 582 (2005) 230–240.
[64] G.M. Brisard, A.P.M. Camargo, F.C. Nart, T. Iwasita, Electrochem. Commun. 3 (2001) 603–607.
[65] C.K. Kuo, N.D. Patel, A. Tan, P. Sarkar, P.S. Nicholson, Solid State Ionics 53–56 (1992) 564–570.
[66] J. Wu, M. Saito, M. Takeuchi, T. Watanabe, Appl. Catal. A 218 (2001) 235–240.
[67] W. Hua, W. Li, S. Xuelian, Coal Chem. Ind. 33 (2005) 30–35.
[68] Z. Huo, M. Hu, X. Zeng, J. Yun, F. Jin, Catal. Today 194 (2012) 25–29.
[69] M. Xu, M.J.L. Gines, A.M. Hilmen, B.L. Stephens, E. Iglesia, J. Catal. 171 (1997) 130–147.
[70] A. Basonde, B. Tidona, P.R. von Rohr, A. Urakawa, Catal. Sci. Technol. 3 (2013) 767–778.
[71] M. Kasaie, M. Sohrabi, J. Mex. Chem. Soc. 53 (2009) 233–238.